Validation and identification of anoikis-related lncRNA signatures for improving prognosis in clear cell renal cell carcinoma

Zhenjie Zhu[1], Qibo Wang[1], Xiaowei Zeng[1], Shaoxing Zhu[2], Jinchao Chen[1]

[1]Zhejiang Cancer Hospital, Institute of Basic Medicine and Cancer (IBMC), Chinese Academy of Sciences, Hangzhou, China
[2]Fujian Medical University Union Hospital, Fuzhou, China

Correspondence to: Shaoxing Zhu, Jinchao Chen; **email:** zsxing2005@126.com, https://orcid.org/0009-0009-6801-5309; chenjc@zjcc.org.cn

ABSTRACT

Background: Clear cell carcinoma (ccRCC) usually has a high metastasis rate and high mortality rate. To enable precise risk stratification, there is a need for novel biomarkers. As one form of apoptosis, anoikis results from the disruption of cell-cell connection or cell-ECM attachment. However, the impact of anoikis-related lncRNAs on ccRCC has not yet received adequate attention.
Methods: The study utilized univariate Cox regression analysis in order to identify the overall survival (OS) associated anoikis-related lncRNAs (ARLs), followed by the LASSO algorithm for selection. On this basis, a risk model was subsequently established using five anoikis-related lncRNAs. To dig the inner molecular mechanism, KEGG, GO, and GSVA analyses were conducted. Additionally, the immune infiltration landscape was estimated using the ESTIMATE, CIBERSORT, and ssGSEA algorithms.
Results: The study constructed a novel risk model based on five ARLs (AC092611.2, AC027601.2, AC103809.1, AL133215.2, and AL162586.1). Patients categorized as low-risk exhibited significantly better OS. Notably, the study observed marked different immune infiltration landscapes and drug sensitivity by risk stratification. Additionally, the study preliminarily explored potential signal pathways associated with risk stratification.
Conclusion: The study exhibited the crucial role of ARLs in the carcinogenesis of ccRCC, potentially through differential immune infiltration. Furthermore, the established risk model could serve as a valuable stratification factor for predicting OS prognosis.

INTRODUCTION

In 2018, about 403,000 cases of renal cancer were newly diagnosed worldwide, bringing huge challenges to public health and serious socio-economic burden [1, 2]. As a heterogeneous tumor, clear cell carcinoma (ccRCC) accounts for 80% of renal cell carcinoma [3]. Different from advanced ccRCC, patients with early diagnosis and treatment have a better prognosis [2]. Although many cancer biomarkers have been discovered, their accuracy in predicting the prognosis of patients has not been clinically recognized and applied.

The mining of biomarkers can improve the efficiency of diagnosis and the efficacy of cancer treatment.

Anoikis is one apoptosis form due to disruption of cell-ECM attachment or cell-cell connection [4]. Under physiological conditions, anoikis eliminates misplaced or shed cells and contributes to tissue homeostasis. Under pathological conditions, anoikis is involved many pathological processes including tumorigenesis. By dissociating from the ECM and avoiding systemic apoptosis in the process, cancer cells eventually spread, thus loss of opportunity for surgery [4]. This process

involves genetic and molecular changes that allow cells to survive without ECM attachment [5]. Recent studies have shown that anoikis has potential therapeutic value in RCC. Some anoikis key genes was reported to promote proliferation and migration in RCC [6]. In addition, progression of RCC can be inhibited by reversing anoikis resistance [7]. Quinazolines activates anoikis by AKT signal pathway adjustment, leading to an antitumor effect [8]. Anoikis resistance is one key characteristic of metastatic tumor cells. However, as a tumor prone to hematogenous metastasis, the mechanism of anoikis in ccRCC is not fully studied. Multiple biological functions of ccRCC are regulated by ECM by providing adhesion substrates and modulating signal transduction, including proliferation, angiogenesis and invasion [9]. There is evidence that increased anoikis activity can reduce the invasive ability of ccRCC cancer cells through regulation of key protein expression levels [10]. All these evidences indicate the potential role of anoikis in ccRCC.

The immune microenvironment (TME) plays a critical role in ccRCC carcinogenesis. The dynamic and complex role of TME includes both immunostimulation and immunosuppression [11]. Tumor-infiltrating lymphocytes (TILs) are associated with a favorable prognosis for ccRCC. The antitumor immune-response can be inhibited by the high density of myeloid-derived suppressor cells (MDSC) in ccRCC [12]. In addition, tumor-associated macrophages (TAM) as well as cancer-associated fibroblasts (CAF) also participated in the shaping of TME [13]. Due to the important role of TME, the treatment regimen that targets TME-related groups also has positive clinical value [14]. Immuno-related therapies have achieved initial efficacy in clinical trials of ccRCC [13]. Further exploration of immune-related pathways and related targets is of great significance.

Long non-coding RNA (lncRNA), as a type of RNA that exists in the nucleus or cytoplasm, has a transcript length of more than 200nt [15]. LncRNAs have been shown to be involved in many important gene expression regulation processes, including chromatin modification, transcriptional interference, DNA methylation and histone modification [16]. Increasing evidence showed in the development of RCC, lncRNAs interact with a variety of RNAs and proteins at transcription, post-transcription and epigenetic level, which further leads to the involvement of RCC invasion and metastasis [17–20]. According to the 2021 review, anoikis-related lncRNAs including ANRIL, FOXD2-AS1, HOTAIR, and SNHG12 have been unveiled to participate in the process of tumor metastasis, stem cell formation and tumor survival [4]. In addition, the combination of chemotherapy drugs and specific lncRNAs can improve

the therapeutic effect [21, 22]. Therefore, risk stratification based on lncRNA has a clinical value. However, the research of anoikis-related lncRNAs in ccRCC in insufficient.

To dig the role of anoikis-related lncRNAs (ARLs) in ccRCC, we built a novel risk signature based on 5 ARLs and verified its effectiveness in predicting the prognosis of patients with ccRCC. Immune microenvironment differences by risk stratification were comprehensively analyzed. Differences in immune response and drug sensitivity by risk stratification were also further explored. In view of the rapid development of targeted drugs in ccRCC treatment [23], our study provides idea for further finding the ideal target responsible for disease development and clinical application potential.

MATERIALS AND METHODS

Data download

The open transcriptome matrix and clinicopathological characteristic information were collected from TCGA. After excluding samples with no effective survival time, 525 samples were included for analysis. The gene expression matrix was extracted by Perl scripts. The ensemble human genome browser GRCh38. p13 was utilized to annotate the symbol of mRNA and lncRNA.

Identification of anoikis-related lncRNAs (ARLs)

From the MSigDB database, 34 anoikis-related genes (ARGs) were obtained (Supplementary Table 1). Pearson correlation analysis was set at a threshold of |correlation coefficient (r) | > 0.6, and $P < 0.001$ [24]. Then, 44 lncRNAs were identified as ARLs for analysis (Supplementary Table 2).

ARLs risk model establishment

On the basis of univariate-LASSO Cox algorithm to identify the overall survival (OS) related ARLs, the risk score = (0.683 x AL162586.1) + (-0.753 x AC027601.2) + (-0.993 x AC103809.1) + (1.679 x AL133215.2) + (-0.414 x AC092611.2). The median of risk score is used to stratify risk. The Kaplan-Meier survival curve was utilized by R package "survival". The training and test cohort were randomly divided with a ratio of 7:3 [25].

Molecular functional evaluation

The differently expressed genes (DEGs) of ccRCC by risk stratification were identified by algorithm "limma" (|FC| ≥ 2, $P < 0.05$). Metascape database was used to perform DEGs enrichment analysis. The GO analysis and KEGG analysis were estimated via "clusterProfiler" R package [26].

Independent prognosis analysis

Univariate/multivariate Cox analysis were carried out via R package "survival". Algorithm "timeROC" was conducted to evaluate the AUC at 1-, 3-, and 5-years. A nomogram model was constructed via "rms" script. The consistence of OS rate predicted nomogram and actual OS rate was evaluated by calibration diagram.

Consensus clustering analysis of ccRCC

Different molecular subtype clustering from ccRCC samples was done via algorithm "ConsensusClusterPlus" by R language based on the 5 prognostic ARLs. Partitioning around medoids with "euclidean" distances and optimal classification of K = 2-9 were used for clustering process.

Immune microenvironment landscape and drug sensitivity evaluation

The estimate scores were estimated by algorithm "estimate" from R package. CIBERSORT and ssGSEA algorithms from R package were employed to calculate the immune cell proportions. "GSVA" script was used to estimate the immune function score. Immunophenoscore (IPS) results, Immune Dysfunction and Exclusion (TIDE) score and drug sensitivity data were obtained from TCIA database, TIDE database and GDSC database, respectively.

Statistical analysis

All statistical analysis were performed by using the R software (version 4.1.0) and Perl scripts. Wilcoxon rank-sum test and ANOVA were used for the assessment differential functions of two groups and multiple groups, respectively. All statistical significance were set at $P < 0.05$.

RESULTS

Generation of prognostic anoikis-related lncRNAs (ARLs)

As shown in Sankey plot, a total of 44 lncRNAs associated with anoikis-related genes were identified as anoikis-related lncRNAs (ARLs) in this study (Figure 1A and Supplementary Figure 1). By the univariate-LASSO analysis, 10 OS associated ARLs for ccRCC were identified (Figure 1B, 1C). 5 prognostic ARLs were confirmed by multivariate Cox regression analysis to be able to independently predict the OS rate, which further led to the establishment of the ARLs risk model. Correlation analysis results suggested a significant association between the 5 selected ARLs and anoikis-

related genes (Figure 1D). As shown in Figure 1E, the expressions of AL162586.1, AC027601.2, and AC103809.1 were relatively highly expressed in the tumor group, while the expressions of AL133215.2 and AC092611.2 were higher in the normal group.

Construction of ARLs risk model in ccRCC

Since 5 ARLs with ccRCC prognostic value were selected, a novel risk model was further established. Patients with ccRCC were risk stratified according to their ARLs risk scores. The inverse association between the survival time and risk score could be observed (Figure 2A). Heatmap diagram showed the expressions of AC092611.2, AC027601.2, and AC103809.1 were overexpressed in the low-risk group, whereas the expressions of AL133215.2 and AL162586.1 were higher in the other group (Figure 2B). The results of KM survival curve suggested a large advantage in survival for patients for patients with low risk (Figure 2C). The ROC curve results show an AUC value of 0.758 for this novel ARLs risk model (Figure 2D).

Validation of ARLs prognostic signature in ccRCC

An internal validation was subsequently developed to investigate the independence and accuracy of the established ARLs risk model in prognosis evaluating. The training and test cohorts were randomly divided into 525 ccRCC patients in a 7:3 ratio. Patients in the training and test cohorts were then randomly divided into two subgroups. Survival time was demonstrated by scatter plots to be negatively correlated to risk score in both groups (Figure 3A, 3C). In both cohorts, significantly better OS rate could be observed in the low-risk group, which was shown by Kaplan-Meier analysis (Figure 3B, 3D). The results of time ROC curve exhibited the acceptable AUC values at 1-, 3-, and 5-years for both training and test cohort (Figure 3E, 3G). The heatmap diagrams showed that the expressions of AC092611.2, AC027601.2, and AC103809.1 were higher, while the expression of AL133215.2 and AL162586.1 were lower in the low-risk group (Figure 3F, 3H). These results indicate the effectiveness of the established ARLs in predicting the ccRCC prognosis.

Risk scores for different clinicopathological features

The subgroup analysis was subsequently performed. According to the median risk score, patients were stratified according to different clinicopathological features by dichotomy. The OS rate of ccRCC patients in the low-risk group were significantly higher in grade I-II, grade III-IV, male, female, age < 65, age ≥ 65, stage III-IV, N 0, M 0, M 1, T I-II, and T III-IV. However, the OS rate of patients with ccRCC in

stage I-II and N 1 was similar (Figure 4). These results illustrate the established risk score allows prognosis assessment of different clinical features.

Independence analysis of ARLs-based prognostic model of ccRCC

Univariate Cox regression analysis showed in addition to multiple clinical characteristics, risk score was also significantly correlated with ccRCC OS rate (Figure 5A). Multivariate Cox regression analysis further demonstrated risk score as an independent prognostic indicator for ccRCC patients (Figure 5B). We subsequently established nomograms to accurately predict patient survival time (Figure 5C). Calibration curves showed that the OS rates predicted by the

nomogram were consistent with the actual OS rates (Figure 5D). The time dependent ROC curve also yielded acceptable AUC values for 1, 3, and 5 years (Figure 5E). In summary, the independent prognostic significance of ARLs risk model for ccRCC prognosis was confirmed.

Molecular function analysis of ARLs-related risk groups

To investigate the potential molecular mechanism of ARLs risk model, multiple enrichment analysis algorithms were further performed. Volcano diagram illustrated the DEGs by risk stratification, showing in the high-risk group, most of the DEGs were significantly upregulated (Figure 6A). Subsequently
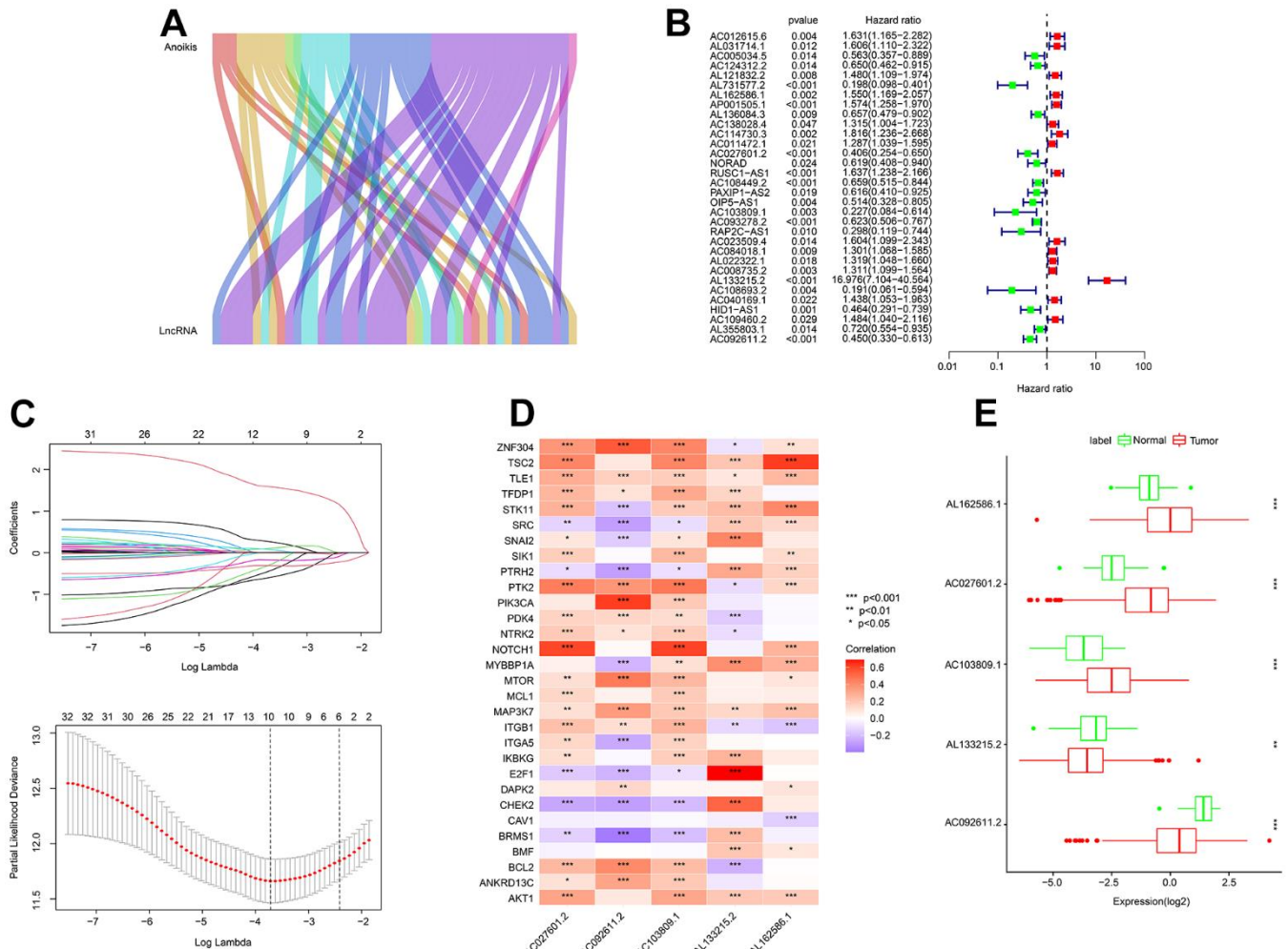

Figure 1. Identification of prognostic ARLs. (**A**) Identification of lncRNAs associated with anoikis-related genes by the Sankey diagram. (**B**, **C**) Prognostic ARLs identification via univariate-LASSO analysis. (**D**) Correlation analysis of the prognostic ARLs and ARGs. (**E**) The expression profiler of prognostic ARLs in the normal and tumor groups.
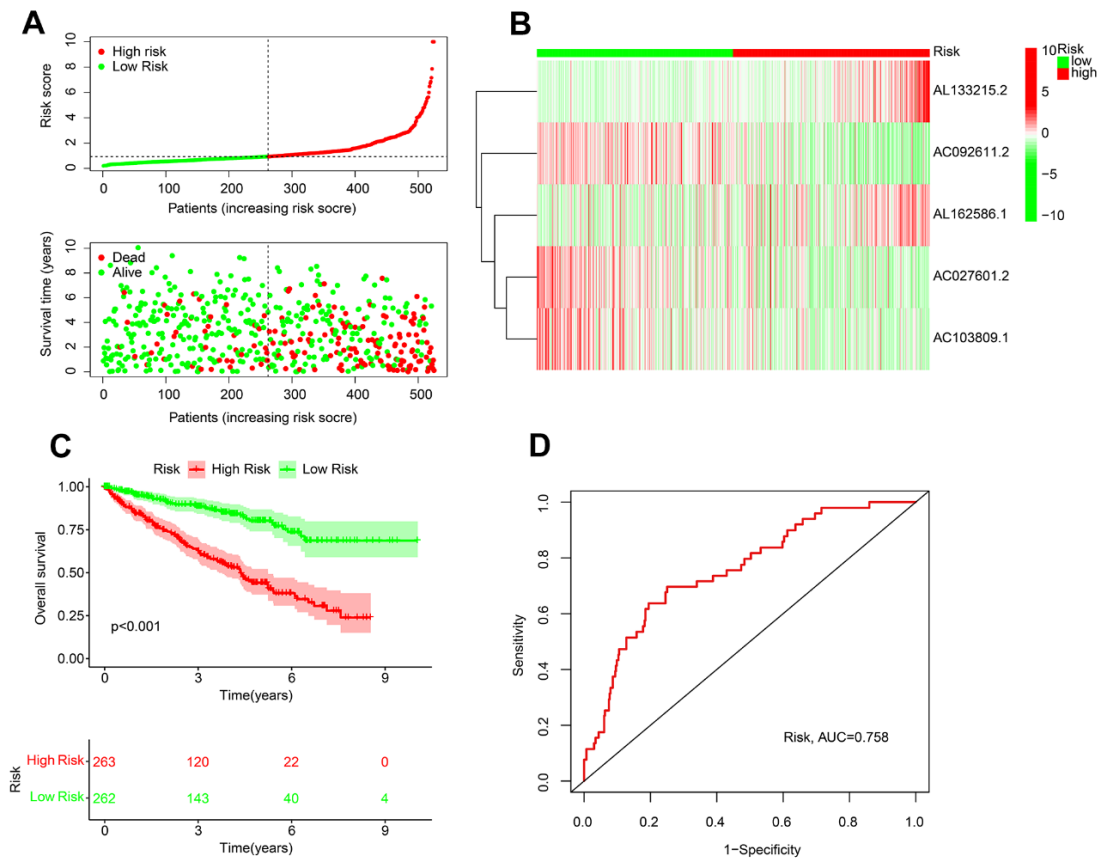
Figure 2. Risk model establishment of the prognostic ARLs in ccRCC. (**A**) Distribution plot of the risk score and correlation analysis of the survival time and risk score of ccRCC patients. (**B**) The expression of prognostic ARLs in ARLs score subgroup. (**C**) Kaplan-Meier survival curve of ccRCC patients in ARLs score subgroup. (**D**) ROC curve of risk model, and the AUC was 0.756.
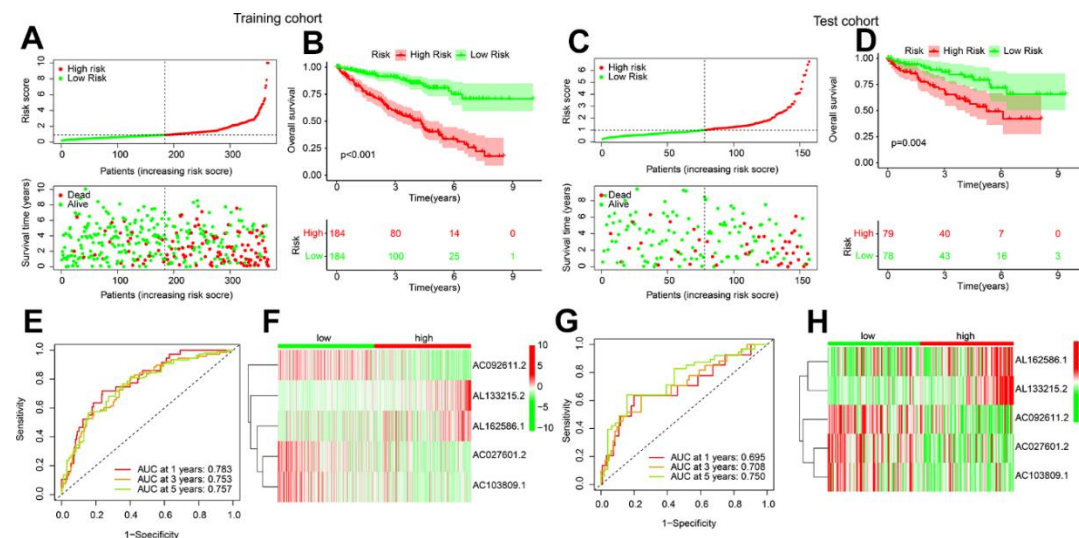

Figure 3. Validation of risk model in training cohort and test cohort. (**A**) Distribution of the risk score and correlation analysis of survival time and risk score in training cohort. (**B**) Kaplan-Meier survival curve of ccRCC patients with in the low- and high-risk group in training cohort. (**C**) Distribution of the risk score and correlation analysis of survival time and risk score in test cohort. (**D**) Kaplan-Meier survival curve of ccRCC patients with in the low- and high-risk group in test cohort. (**E**—**H**) ROC curve analysis and the expression of 5 ARLs in low- and high-risk group in training and test cohort.

performed enrichment analysis result suggested the DEGs were significantly enriched in some immune related signaling pathways, such as adaptive immune response and phagocytosis, recognition (Figure 6B). KEGG enrichment analysis illustrated that cytokine−cytokine receptor interaction was enriched (Figure 6C). Enriched immune related biological processes could be observed by GO enrichment analysis, including defense response to bacterium, positive regulation of lymphocyte activation and humoral immune response (Figure 6D). These results suggested the role of immune-associated signaling pathways in mediating ARL-related functions.

Characteristic of molecular subtypes and immune microenvironment analysis

Based on the selected 5 ARLs, consensus clustering was performed for ccRCC subtype clustering. The heat map shows the optimal classification when K = 3, with classes A, B and C having 154, 166 and 205 samples respectively (Figure 7A). Survival curve exhibited that class B patients had the most optimistic OS rate (Figure 7B). The principal component analysis score plot illustrated a clear separation of among three groups

(Figure 7C). ESTIMATE algorithm results suggested that Cluster B patients had higher tumor purity than the other two groups; however, the immune and ESITMATE score were lower (Figure 7D–7F).

In addition, more efforts were made to estimate the component of immune cells in the different subtypes. The result of CIBERSORT showed that Cluster C patients had higher infiltration level of plasma cells, CD8$^+$ T cells, follicular helper T cells, regulatory T cells (Tregs) and M0 macrophages, whereas the infiltration level of resting CD4$^+$ memory T cells, monocytes, resting NK cells, and M2 macrophages were lower (Figure 7G). ssGSEA algorithm result suggested Cluster C had significantly higher portions of immune cells in comparison to those in Cluster A and B (Figure 7H). These findings demonstrate that different ccRCC molecular subtypes were closely related to patient prognosis as well as immune infiltration.

Association of ARLs risk model and immune microenvironment landscape

The immune microenvironment landscape of patients by risk stratification was further evaluated. High-risk score
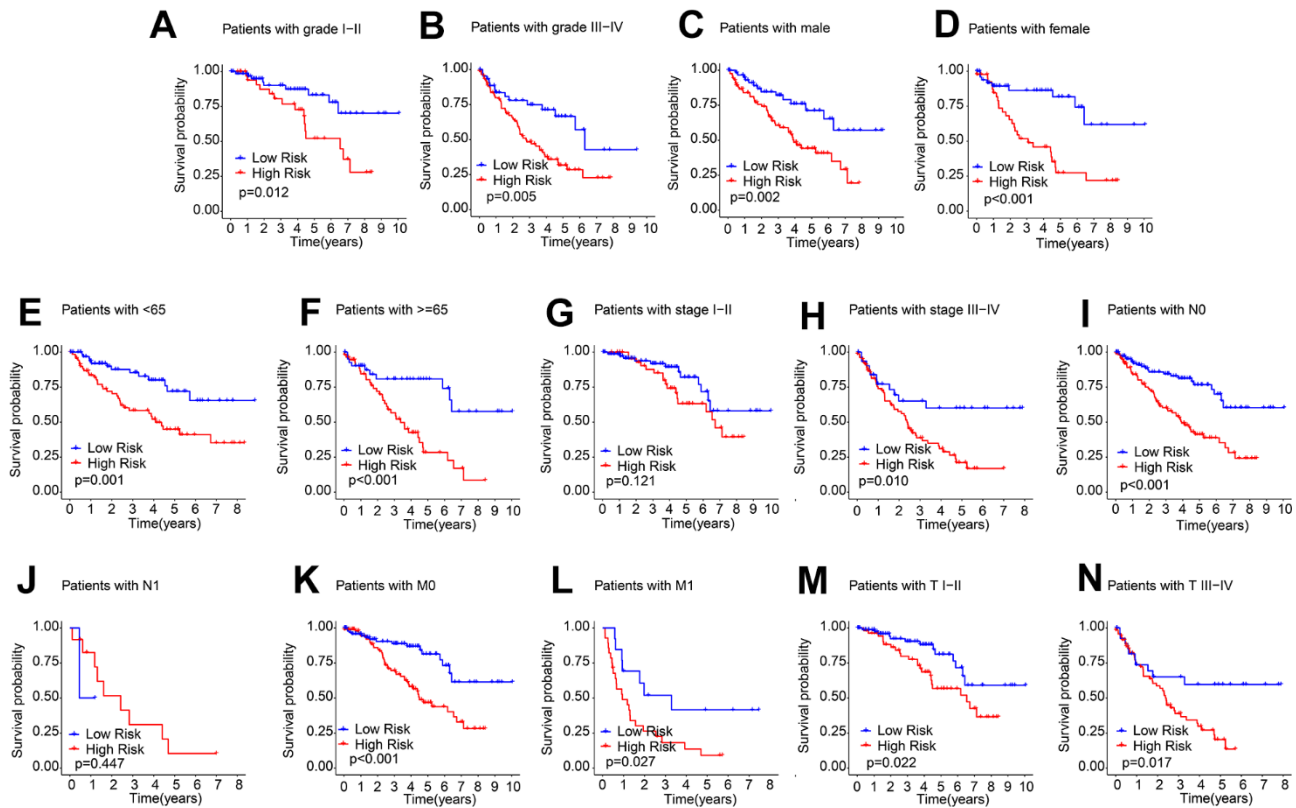

Figure 4. Prognostic analysis of ARLs score in different clinical features. The prognostic KM curve of ccRCC samples among the (**A**) Grade I-II; (**B**) Grade III-IV; (**C**) Male; (**D**) Female; (**E**) Age < 65; (**F**) Age ≥ 65; (**G**) Stage I-II; (**H**) Stage III-IV; (**I**) N0; (**J**) N1; (**K**) M0; (**L**) M1; (**M**) T I-II; (**N**) T III-IV.

patients had higher ESTIMATE level, immune score level and lower tumor purity level (Figure 8A–8C). Subsequent result showed lower TIDE scores could be observed in the low-risk score patients, indicating better outcomes of immunotherapy response for ccRCC (Figure 8D). CIBERSORT result indicated that the proportion of naïve B cells, monocytes, resting CD4^{+} memory T cells, resting NK cells, M2 macrophages, resting and activated dendritic cells were significantly higher for low-risk patients, while memory B cells, plasma cells, CD8^{+} T cells, TfH cells, M0 and M1 macrophages, Tregs and activated NK cells, were higher for high-risk score patients (Figure 8E). ssGSEA algorithm result indicated that the proportion of eosinophil, mast cell, immature dendritic cell and neutrophil were higher in the low-risk group, whereas the fraction of activated B, CD4^{+} T, CD8^{+} T and dendritic cells, as well as MDSC and TfH cell were higher in the high-risk group (Figure 8F).
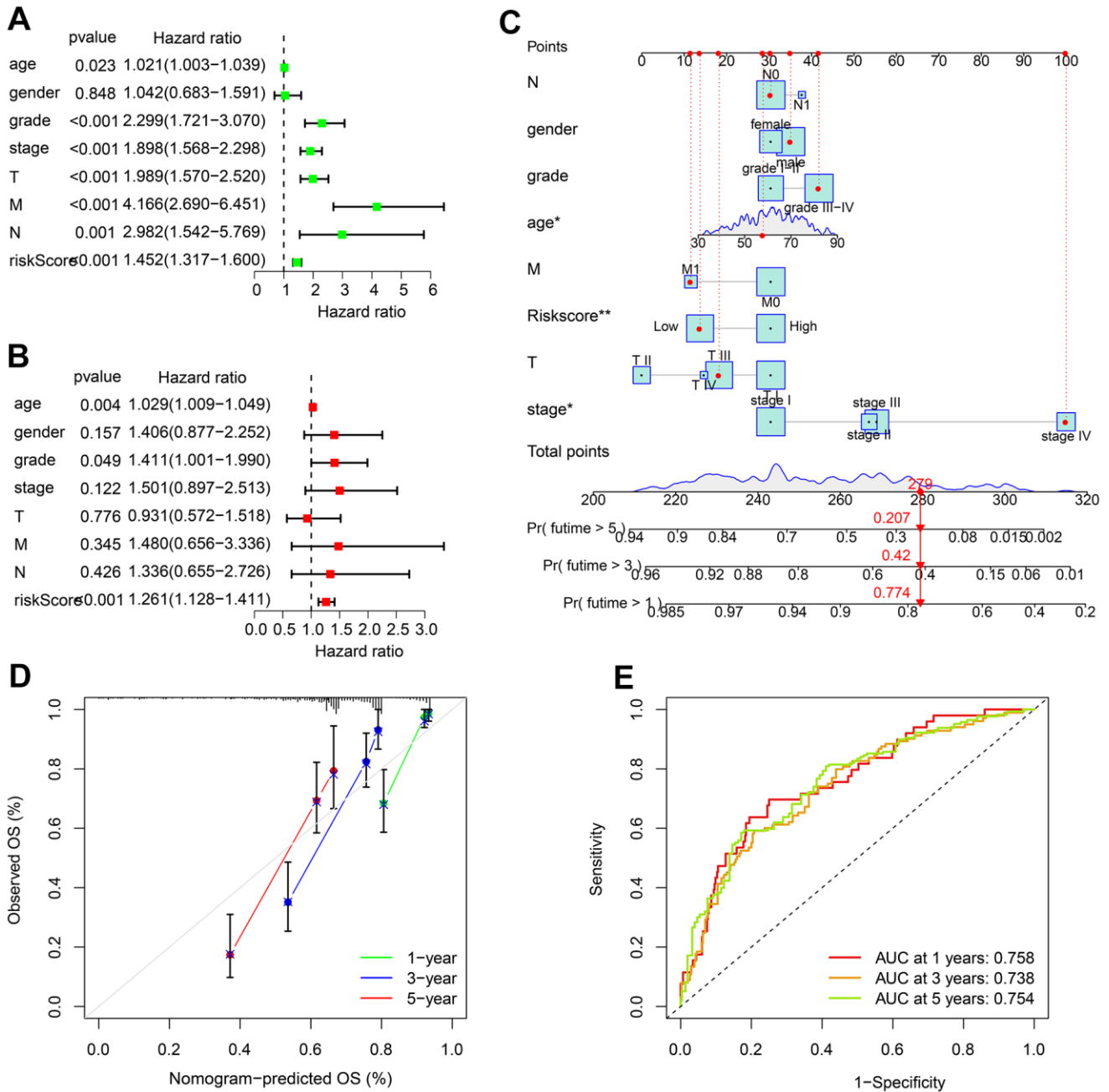

Figure 5. Independence evaluation of ARLs risk model. (**A**) Univariate and (**B**) multivariate analysis reveals the independence of ARLs score and clinical features of ccRCC. (**C**) Nomogram model constructed based on the ARLs risk model and clinicopathological characteristics. (**D**) Calibration curve shows the consistency of the OS rate predicted by nomogram. (**E**) Time-dependent ROC curve.

Considering the remarkable difference in immune microenvironment by risk stratification, the response of immunotherapy was further evaluated. IPS results illustrated that high-risk score might lead to better response to immune checkpoint inhibitor-related therapy (Figure 8G, 8H). Immune function result showed that most of immune score were higher in patients with high-risk, whereas the type II IFN response level was lower (Figure 8I). The above result showed the ARLs risk model was closely associated with immune infiltration, and there may be differences in immunotherapy response in the ARL risk stratification.

Drug sensitivity analysis of different risk groups

Targeted drug therapy and chemotherapy has been considered as vital strategies in ccRCC clinical management. Thereafter, the sensitivity differences to several potential antineoplastic drugs by risk scoring stratification were evaluated. As shown in Figure 9A–9H, Sorafenib and Erlotinib had higher IC50 in the low-risk group; while high risk score patients had significantly higher IC50 of Sunitinib, Saracatinib, Paclitaxel, Dasatinib, Imatinib, and Rapamycin.

Correlation analysis suggested that the risk score was negatively associated with IC50 of Sorafenib and Erlotinib, whereas positively associated with IC50 of Sunitinib, Dasatinib, Saracatinib, Imatinib, Paclitaxel and Rapamycin (Figure 9I–9P).

DISCUSSION

In this study, a ARLs prognostic model of for ccRCC patients was established and its effectiveness was successfully verified. Among the five lncRNAs we screened, AC092611.2 and AC027601.2 were reported as prognostic markers in ccRCC [27, 28]. AL162586.1, ac103809.1 and AL133215.2 have not been reported. In RCC, many carcinogenic lncRNAs were overexpressed, while many tumors suppressor lncRNAs were down-regulated [29, 30]. A variety of lncRNAs have been screened to be critical for the progression of RCC and serve as markers of poor prognosis in patients [20, 31, 32]. In addition, the impact of some lncRNAs on the immune response of RCC has been suggested in the literature. LINC00973 was reported to increase the expression of siglec-15, which is a cancer cell surface antigen [33]. In terms of molecular mechanisms, the activation of multiple signaling pathways in RCC,
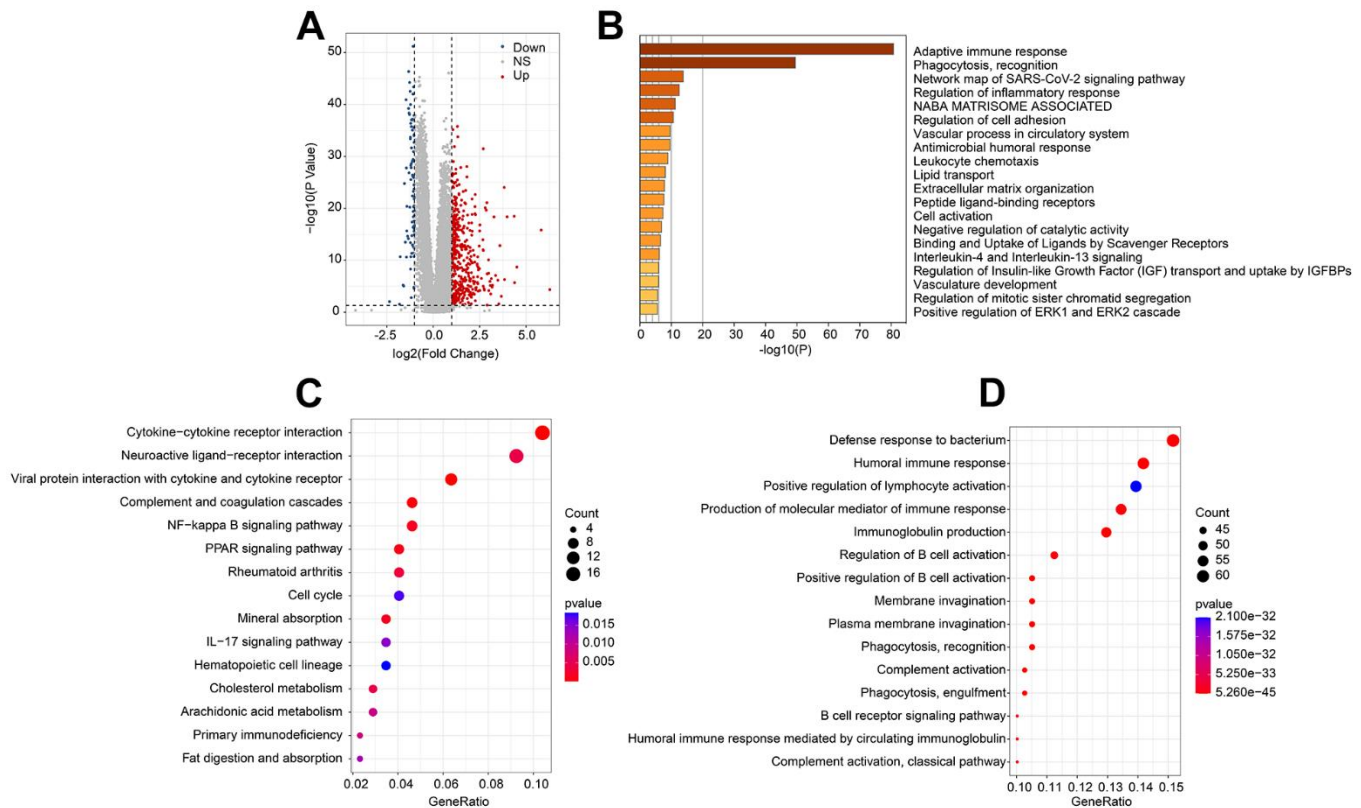

Figure 6. Molecular functional analysis of ARLs score subgroups. (**A**) Generation of the DEGs of ARLs score subgroups. (**B**) Enrichment analysis of DEGs. (**C**) KEGG and (**D**) GO enrichment analysis of ARLs score subgroups.
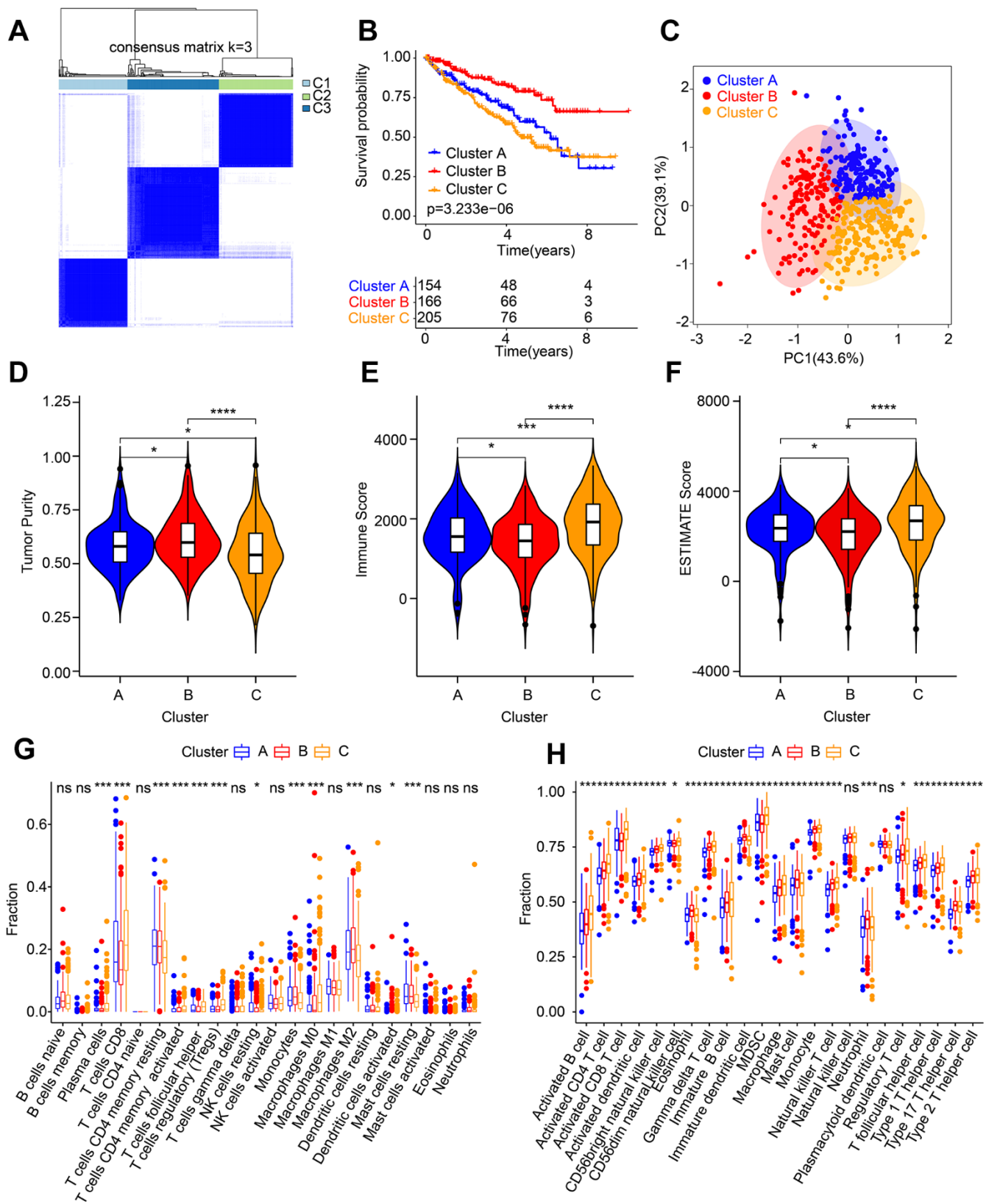
Figure 7. Molecular subtypes analysis and immune microenvironment landscape characterization. (**A**) Identification of the molecular subtypes for ccRCC. (**B**) Clinical prognostic analysis of Cluster A, Cluster B and Cluster C. (**C**) PCA score plot shows a significant distribution pattern of patients in Cluster A, Cluster B and Cluster C. (**D**–**F**) Tumor purity, immune and ESTIMATE scores. The proportion of immune cells calculated by (**G**) CIBERSORT and (**H**) ssGSEA.
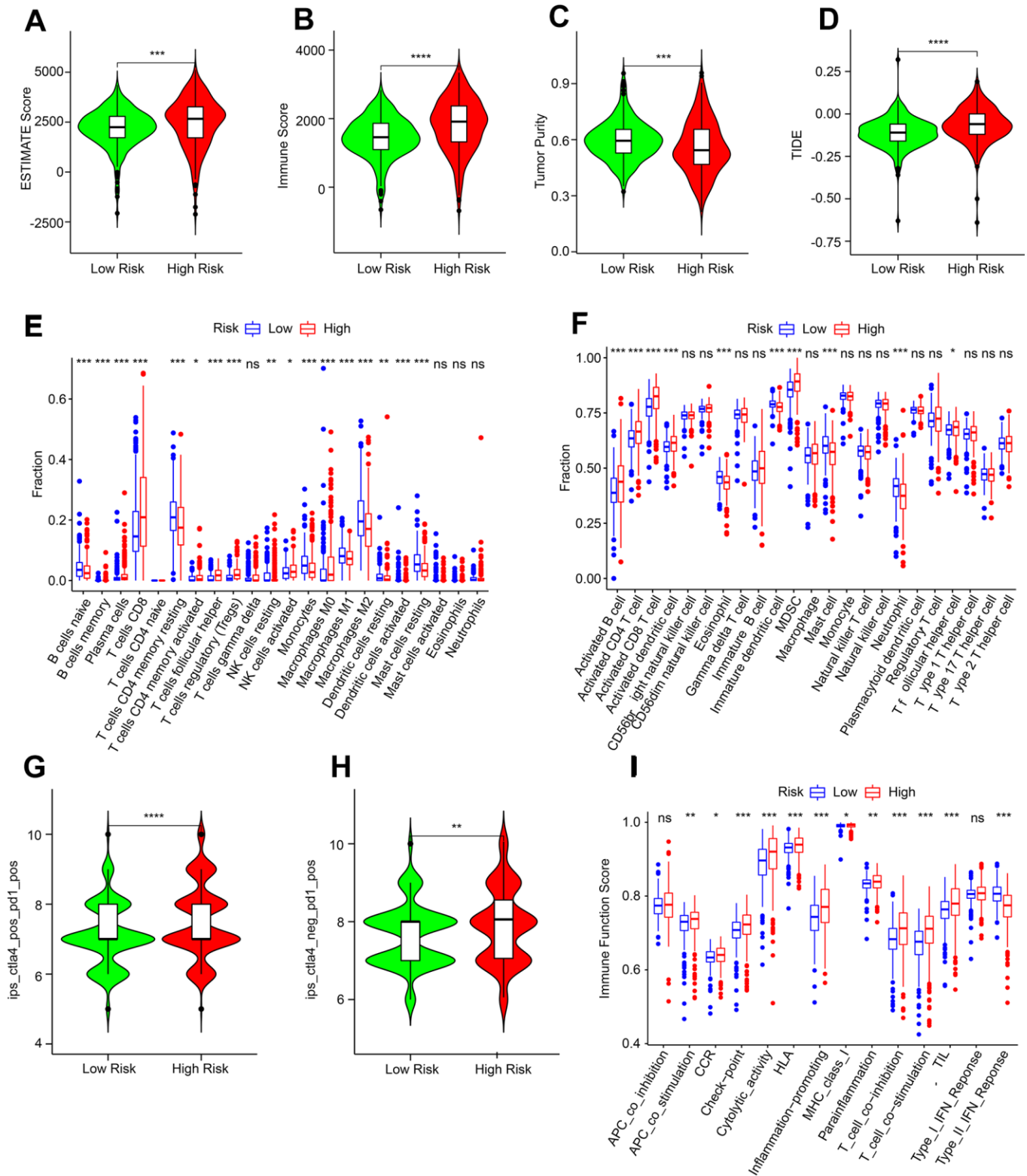
Figure 8. Immune infiltration characterization of ARLs scores subgroups. (**A**–**C**) ESTIMATE, immune scores and tumor purity. (**D**) TIDE score. (**E**, **F**) CIBERSORT and ssGSEA algorithm to estimate the immune cells fraction of ARLs score subgroups. (**G**, **H**) IPS score. (**I**) Immune function score.

including epithelial-mesenchymal transition process, hedgehog, PI3K/AKT and the VEGF signaling have been shown to be associated with lncRNA [34]. LncRNA has been reported to affect tumor development through anoikis process [35]. Our results further illustrate the role of lncRNAs in RCC and provide new research targets.

Our results of pathway enrichment analysis illustrated that our prognostic typing was closely correlated with immune-related pathways including adaptive immune response and phagocytosis. As an important part of anoikis process, ECM is associated with immunity in tumor development [36]. Traditionally, the ECM was thought to serve only as a scaffolding, but recently, its
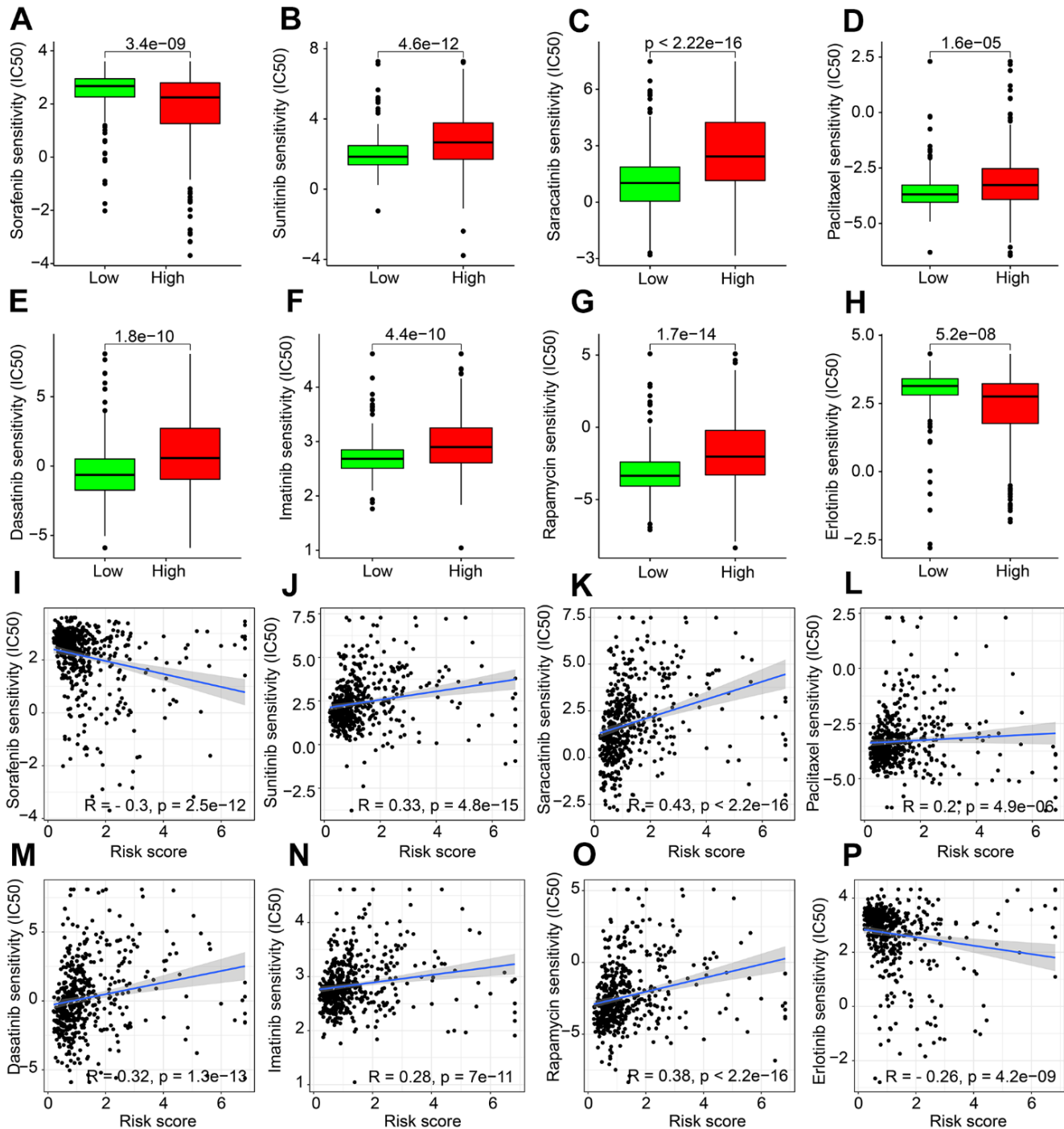

Figure 9. Drug sensitivity exploration. The distribution of IC50 in (**A**) Sorafenib. (**B**) Sunitinib. (**C**) Saracatinib. (**D**) Paclitaxel. (**E**) Dasatinib. (**F**) Imatinib. (**G**) Rapamycin. (**H**) Erlotinib. (**I**–**P**) Correlation analysis of ARLs prognostic signature and drug sensitivity (IC50).

role in carcinogenesis has become increasingly clear. The ECM physical properties, such as ECM porosity, rigidity and insolubility can affect the biological functions of resident cells including the formation of immune microenvironment [36, 37]. There is already evidence that ECM rigidity strongly affects T-cell biological functions including activation, proliferation and differentiation [38]. In the tumor microenvironment, elevated hypoxia and metabolic stress could lead by poor diffusion of tumor ECM, leading to upregulation of TGF-β and VEGFA, which are commonly considered as immunosuppressive factors [39, 40]. ECM is also involved in tumor-related inflammatory responses, such as the polarization of tumor-associated macrophages (TAM), which makes macrophages biased toward M1 polarization and enhances the cytotoxic activity of macrophages against tumor cells [41]. Our data also showed a strong correlation between ECM-associated anoikis and immunity. The specific functions and underlying mechanisms of ECM-associated anoikis in tumor-related immunity need to be further explored.

Our results suggest a correlation between anoikis and response to immunotherapy. Although no association of anoikis with tumor immunotherapy has been reported so far, ECM has been reported to be involved in the antitumor immunotherapy process. During carcinogenesis process, the structure, physical properties and metabolism of ECM are highly dysregulated [42]. The ECM in tumoral cells is at least 1.5 times more rigid than the extracellular matrix in normal tissues [43]. On this basis, cell-ECM adhesion in tumor tissues is enhanced and cell-cell contact is disrupted, leading to tumor growth and metastasis [44]. The expression of PD-L1 is crucial to the immune escape process of tumor cells [45]. PD-L1 expression can be elevated through the regulatory mechanism of rigid ECM on actin, leading to immune system escape and tumor growth [46, 47]. Rigid ECM may also act as a physical barrier to T cell infiltration and localization; therefore, the anti-tumor immune behavior is disturbed [48]. In contrast, loose regions of glycoproteins and collagen in the ECM tend to promote T cell motility [49]. In addition, during T cell activation, an increase in HA binding capacity enhances T cells to roll on HA substrates, leading to better T cell migration and extravasation [50]. In addition, ECM can regulate DC maturation. Exposure to HA fragments can regulate the level of DC activation, thereby regulating the process of cancer antigen presentation [51]. At the same time, the density of tumor ECM can regulate the distribution of drugs and immune cell infiltration in tumors [52]. Based on the above findings, ECM has become one of the popular anticancer targets [53]. Targeting both collagen and hyaluronic acid in ECM has been reported [54]. Highly expressed collagen is associated with poor overall survival and

affects response to chemotherapy, radiotherapy, and immunotherapy [55]. Drugs coupled with collagen-binding antibody fragments targeted to tumors with collagen-rich ECM resulted in a more durable antitumor effect in tumors [56]. A kind of hyaluronidase named PEGPH20, has been shown to successfully degrade HA in tumors and reshape tumor stroma through modulation of ECM components, thereby improving perfusion and drug delivery [57]. Further studies of ECM and anoikis have potential clinical applications.

Our study for sure has shortcomings. The analysis in this paper is correlation analysis without causal analysis, so the value of anoikis cannot be further analyzed. This paper lacks experimental data support, and further *in vitro* or *in vivo* experiments will better verify the conclusions of this paper. In addition, our results showed high-risk patients benefit more from immune-related therapy. However, we did not find any evidence of patients receiving immunotherapy in the public database. Stratified correlation analysis of real-world ccRCC immunotherapy response and risk stratification will have positive clinical significance. In conclusion, our data demonstrate the predictive value of anoikis-associated lncRNA prognostic models for patients with ccRCC.

AUTHOR CONTRIBUTIONS

ZZ and QW contributed the data collection and data analysis. XZ and JC conceived the original ideas and composed this manuscript. SZ contributed the table and figures of this manuscript. All authors contributed to the article and approved the submitted version.

CONFLICTS OF INTEREST

The authors declare that they have no conflicts of interest.

FUNDING

REFERENCES

1. Znaor A, Lortet-Tieulent J, Laversanne M, Jemal A, Bray F. International variations and trends in renal cell carcinoma incidence and mortality. Eur Urol. 2015; 67:519–30.
   https://doi.org/10.1016/j.eururo.2014.10.002
   PMID:25449206

2. Bray F, Ferlay J, Soerjomataram I, Siegel RL, Torre LA, Jemal A. Global cancer statistics 2018: GLOBOCAN

estimates of incidence and mortality worldwide for 36 cancers in 185 countries. CA Cancer J Clin. 2018; 68:394–424.
https://doi.org/10.3322/caac.21492 PMID:30207593

3. Hsieh JJ, Purdue MP, Signoretti S, Swanton C, Albiges L, Schmidinger M, Heng DY, Larkin J, Ficarra V. Renal cell carcinoma. Nat Rev Dis Primers. 2017; 3:17009.
https://doi.org/10.1038/nrdp.2017.9 PMID:28276433

4. Adeshakin FO, Adeshakin AO, Afolabi LO, Yan D, Zhang G, Wan X. Mechanisms for Modulating Anoikis Resistance in Cancer and the Relevance of Metabolic Reprogramming. Front Oncol. 2021; 11:626577.
https://doi.org/10.3389/fonc.2021.626577 PMID:33854965

5. Kakavandi E, Shahbahrami R, Goudarzi H, Eslami G, Faghihloo E. Anoikis resistance and oncoviruses. J Cell Biochem. 2018; 119:2484–91.
https://doi.org/10.1002/jcb.26363 PMID:28836703

6. Gan L, Xiao Q, Zhou Y, Fu Y, Tang M. Role of anoikis-related gene PLK1 in kidney renal papillary cell carcinoma: a bioinformatics analysis and preliminary verification on promoting proliferation and migration. Front Pharmacol. 2023; 14:1211675.
https://doi.org/10.3389/fphar.2023.1211675 PMID:37456749

7. Wang L, Li C, Wang J, Yang G, Lv Y, Fu B, Jian L, Ma J, Yu J, Yang Z, Wu P, Li G, Liu X, et al. Transformable ECM Deprivation System Effectively Suppresses Renal Cell Carcinoma by Reversing Anoikis Resistance and Increasing Chemotherapy Sensitivity. Adv Mater. 2022; 34:e2203518.
https://doi.org/10.1002/adma.202203518 PMID:36004775

8. Sakamoto S, Schwarze S, Kyprianou N. Anoikis disruption of focal adhesion-Akt signaling impairs renal cell carcinoma. Eur Urol. 2011; 59:734–44.
https://doi.org/10.1016/j.eururo.2010.12.038 PMID:21269758

9. Wang Z, Wang K, Gao X, Liu Z, Xing Z. Comprehensive analysis of the importance of PLAUR in the progression and immune microenvironment of renal clear cell carcinoma. PLoS One. 2022; 17:e0269595.
https://doi.org/10.1371/journal.pone.0269595 PMID:35675366

10. Yu M, Lu B, Liu Y, Me Y, Wang L, Li H. Interference with Tim-3 protein expression attenuates the invasion of clear cell renal cell carcinoma and aggravates anoikis. Mol Med Rep. 2017; 15:1103–8.
https://doi.org/10.3892/mmr.2017.6136 PMID:28112366

11. Monjaras-Avila CU, Lorenzo-Leal AC, Luque-Badillo AC, D'Costa N, Chavez-Muñoz C, Bach H. The Tumor Immune Microenvironment in Clear Cell Renal Cell Carcinoma. Int J Mol Sci. 2023; 24:7946.
https://doi.org/10.3390/ijms24097946 PMID:37175653

12. Hakimi AA, Voss MH, Kuo F, Sanchez A, Liu M, Nixon BG, Vuong L, Ostrovnaya I, Chen YB, Reuter V, Riaz N, Cheng Y, Patel P, et al. Transcriptomic Profiling of the Tumor Microenvironment Reveals Distinct Subgroups of Clear Cell Renal Cell Cancer: Data from a Randomized Phase III Trial. Cancer Discov. 2019; 9:510–25.
https://doi.org/10.1158/2159-8290.CD-18-0957 PMID:30622105

13. Kim MC, Jin Z, Kolb R, Borcherding N, Chatzkel JA, Falzarano SM, Zhang W. Updates on Immunotherapy and Immune Landscape in Renal Clear Cell Carcinoma. Cancers (Basel). 2021; 13:5856.
https://doi.org/10.3390/cancers13225856 PMID:34831009

14. Huang Y, Sun H, Guo P. Research Progress of Tumor Microenvironment Targeted Therapy for Clear Cell Renal Cell Carcinoma. Cancer Control. 2023; 30:10732748231155700.
https://doi.org/10.1177/10732748231155700 PMID:36772805

15. Chen YF, Li YJ, Chou CH, Chiew MY, Huang HD, Ho JH, Chien S, Lee OK. Control of matrix stiffness promotes endodermal lineage specification by regulating SMAD2/3 via lncRNA LINC00458. Sci Adv. 2020; 6:eaay0264.
https://doi.org/10.1126/sciadv.aay0264 PMID:32076643

16. Balas MM, Hartwick EW, Barrington C, Roberts JT, Wu SK, Bettcher R, Griffin AM, Kieft JS, Johnson AM. Establishing RNA-RNA interactions remodels lncRNA structure and promotes PRC2 activity. Sci Adv. 2021; 7:eabc9191.
https://doi.org/10.1126/sciadv.abc9191 PMID:33853770

17. Kulkarni P, Dasgupta P, Hashimoto Y, Shiina M, Shahryari V, Tabatabai ZL, Yamamura S, Tanaka Y, Saini S, Dahiya R, Majid S. A lncRNA TCL6-miR-155 Interaction Regulates the Src-Akt-EMT Network to Mediate Kidney Cancer Progression and Metastasis. Cancer Res. 2021; 81:1500–12.
https://doi.org/10.1158/0008-5472.CAN-20-0832 PMID:33500248

18. Lorenzen JM, Thum T. Long noncoding RNAs in kidney and cardiovascular diseases. Nat Rev Nephrol. 2016; 12:360–73.
https://doi.org/10.1038/nrneph.2016.51 PMID:27140855

19. Zhai W, Sun Y, Guo C, Hu G, Wang M, Zheng J, Lin W, Huang Q, Li G, Zheng J, Chang C. LncRNA-SARCC

suppresses renal cell carcinoma (RCC) progression via altering the androgen receptor(AR)/miRNA-143-3p signals. Cell Death Differ. 2017; 24:1502–17. https://doi.org/10.1038/cdd.2017.74 PMID:28644440

20. Hirata H, Hinoda Y, Shahryari V, Deng G, Nakajima K, Tabatabai ZL, Ishii N, Dahiya R. Long Noncoding RNA MALAT1 Promotes Aggressive Renal Cell Carcinoma through Ezh2 and Interacts with miR-205. Cancer Res. 2015; 75:1322–31. https://doi.org/10.1158/0008-5472.CAN-14-2931 PMID:25600645

21. Pedini F, De Luca G, Felicetti F, Puglisi R, Boe A, Arasi MB, Fratini F, Mattia G, Spada M, Caporali S, Biffoni M, Giuliani A, Carè A, Felli N. Joint action of miR-126 and MAPK/PI3K inhibitors against metastatic melanoma. Mol Oncol. 2019; 13:1836–54. https://doi.org/10.1002/1878-0261.12506 PMID:31115969

22. Wang C, Li T, Yan F, Cai W, Zheng J, Jiang X, Sun J. Effect of simvastatin and microRNA-21 inhibitor on metastasis and progression of human salivary adenoid cystic carcinoma. Biomed Pharmacother. 2018; 105:1054–61. https://doi.org/10.1016/j.biopha.2018.05.157 PMID:30021341

23. Rini BI, Campbell SC, Escudier B. Renal cell carcinoma. Lancet. 2009; 373:1119–32. https://doi.org/10.1016/S0140-6736(09)60229-4 PMID:19269025

24. Shu Q, Zhou Y, Zhu Z, Chen X, Fang Q, Zhong L, Chen Z, Fang L. A Novel Risk Model Based on Autophagy-Related LncRNAs Predicts Prognosis and Indicates Immune Infiltration Landscape of Patients With Cutaneous Melanoma. Front Genet. 2022; 13:885391. https://doi.org/10.3389/fgene.2022.885391 PMID:35571053

25. Hu M, Chong R, Liu W, Liu S, Liu X. Characteristic of molecular subtype based on lysosome-associated genes reveals clinical prognosis and immune infiltration of gastric cancer. Front Oncol. 2023; 13:1155418. https://doi.org/10.3389/fonc.2023.1155418 PMID:37197421

26. Yu G, Wang LG, Han Y, He QY. clusterProfiler: an R package for comparing biological themes among gene clusters. OMICS. 2012; 16:284–7. https://doi.org/10.1089/omi.2011.0118 PMID:22455463

27. Li X, Yu H, Wei Z, Gou X, Liang S, Liu F. A Novel Prognostic Model Based on Autophagy-Related Long Non-Coding RNAs for Clear Cell Renal Cell Carcinoma. Front Oncol. 2021; 11:711736.

https://doi.org/10.3389/fonc.2021.711736 PMID:34414116

28. Qi-Dong X, Yang X, Lu JL, Liu CQ, Sun JX, Li C, Wang SG. Development and Validation of a Nine-Redox-Related Long Noncoding RNA Signature in Renal Clear Cell Carcinoma. Oxid Med Cell Longev. 2020; 2020:6634247. https://doi.org/10.1155/2020/6634247 PMID:33425212

29. Wang A, Bao Y, Wu Z, Zhao T, Wang D, Shi J, Liu B, Sun S, Yang F, Wang L, Qu L. Long noncoding RNA EGFR-AS1 promotes cell growth and metastasis via affecting HuR mediated mRNA stability of EGFR in renal cancer. Cell Death Dis. 2019; 10:154. https://doi.org/10.1038/s41419-019-1331-9 PMID:30770799

30. Hong Q, Li O, Zheng W, Xiao WZ, Zhang L, Wu D, Cai GY, He JC, Chen XM. LncRNA HOTAIR regulates HIF-1α/AXL signaling through inhibition of miR-217 in renal cell carcinoma. Cell Death Dis. 2017; 8:e2772. https://doi.org/10.1038/cddis.2017.181 PMID:28492542

31. Trexler M, Bányai L, Patthy L, Pluck ND, Williams RJ. Chemical modification and nuclear magnetic resonance studies on human plasminogen kringle 4. Assignment of tyrosine and histidine resonances to specific residues in the sequence. Eur J Biochem. 1985; 152:439–46. https://doi.org/10.1111/j.1432-1033.1985.tb09216.x PMID:2996892

32. Qi Y, Ma Y, Peng Z, Wang L, Li L, Tang Y, He J, Zheng J. Long noncoding RNA PENG upregulates PDZK1 expression by sponging miR-15b to suppress clear cell renal cell carcinoma cell proliferation. Oncogene. 2020; 39:4404–20. https://doi.org/10.1038/s41388-020-1297-1 PMID:32341409

33. Liu Y, Li X, Zhang C, Zhang H, Huang Y. LINC00973 is involved in cancer immune suppression through positive regulation of Siglec-15 in clear-cell renal cell carcinoma. Cancer Sci. 2020; 111:3693–704. https://doi.org/10.1111/cas.14611 PMID:32780490

34. Braga EA, Fridman MV, Filippova EA, Loginov VI, Pronina IV, Burdennyy AM, Karpukhin AV, Dmitriev AA, Morozov SG. LncRNAs in the Regulation of Genes and Signaling Pathways through miRNA-Mediated and Other Mechanisms in Clear Cell Renal Cell Carcinoma. Int J Mol Sci. 2021; 22:11193. https://doi.org/10.3390/ijms222011193 PMID:34681854

35. Shi T, Zhang C, Xia S. The potential roles and mechanisms of non-coding RNAs in cancer anoikis resistance. Mol Cell Biochem. 2022; 477:1371–80.

https://doi.org/10.1007/s11010-022-04384-6
PMID:35142950

36. Kesh K, Gupta VK, Durden B, Garrido V, Mateo-Victoriano B, Lavania SP, Banerjee S. Therapy Resistance, Cancer Stem Cells and ECM in Cancer: The Matrix Reloaded. Cancers (Basel). 2020; 12:3067.
https://doi.org/10.3390/cancers12103067
PMID:33096662

37. Jurj A, Ionescu C, Berindan-Neagoe I, Braicu C. The extracellular matrix alteration, implication in modulation of drug resistance mechanism: friends or foes? J Exp Clin Cancer Res. 2022; 41:276.
https://doi.org/10.1186/s13046-022-02484-1
PMID:36114508

38. O'Connor RS, Hao X, Shen K, Bashour K, Akimova T, Hancock WW, Kam LC, Milone MC. Substrate rigidity regulates human T cell activation and proliferation. J Immunol. 2012; 189:1330–9.
https://doi.org/10.4049/jimmunol.1102757
PMID:22732590

39. Sanjabi S, Oh SA, Li MO. Regulation of the Immune Response by TGF-β: From Conception to Autoimmunity and Infection. Cold Spring Harb Perspect Biol. 2017; 9:a022236.
https://doi.org/10.1101/cshperspect.a022236
PMID:28108486

40. Gavalas NG, Tsiatas M, Tsitsilonis O, Politi E, Ioannou K, Ziogas AC, Rodolakis A, Vlahos G, Thomakos N, Haidopoulos D, Terpos E, Antsaklis A, Dimopoulos MA, Bamias A. VEGF directly suppresses activation of T cells from ascites secondary to ovarian cancer via VEGF receptor type 2. Br J Cancer. 2012; 107:1869–75.
https://doi.org/10.1038/bjc.2012.468 PMID:23169339

41. Henke E, Nandigama R, Ergün S. Extracellular Matrix in the Tumor Microenvironment and Its Impact on Cancer Therapy. Front Mol Biosci. 2020; 6:160.
https://doi.org/10.3389/fmolb.2019.00160
PMID:32118030

42. Baldari S, Di Modugno F, Nisticò P, Toietta G. Strategies for Efficient Targeting of Tumor Collagen for Cancer Therapy. Cancers (Basel). 2022; 14:4706.
https://doi.org/10.3390/cancers14194706
PMID:36230627

43. Najafi M, Farhood B, Mortezaee K. Extracellular matrix (ECM) stiffness and degradation as cancer drivers. J Cell Biochem. 2019; 120:2782–90.
https://doi.org/10.1002/jcb.27681 PMID:30321449

44. Gkretsi V, Stylianopoulos T. Cell Adhesion and Matrix Stiffness: Coordinating Cancer Cell Invasion and Metastasis. Front Oncol. 2018; 8:145.
https://doi.org/10.3389/fonc.2018.00145
PMID:29780748

45. Sun C, Mezzadra R, Schumacher TN. Regulation and Function of the PD-L1 Checkpoint. Immunity. 2018; 48:434–52.
https://doi.org/10.1016/j.immuni.2018.03.014
PMID:29562194

46. Miyazawa A, Ito S, Asano S, Tanaka I, Sato M, Kondo M, Hasegawa Y. Regulation of PD-L1 expression by matrix stiffness in lung cancer cells. Biochem Biophys Res Commun. 2018; 495:2344–9.
https://doi.org/10.1016/j.bbrc.2017.12.115
PMID:29274784

47. Azadi S, Aboulkheyr Es H, Razavi Bazaz S, Thiery JP, Asadnia M, Ebrahimi Warkiani M. Upregulation of PD-L1 expression in breast cancer cells through the formation of 3D multicellular cancer aggregates under different chemical and mechanical conditions. Biochim Biophys Acta Mol Cell Res. 2019; 1866:118526.
https://doi.org/10.1016/j.bbamcr.2019.118526
PMID:31398408

48. Hartmann N, Giese NA, Giese T, Poschke I, Offringa R, Werner J, Ryschich E. Prevailing role of contact guidance in intrastromal T-cell trapping in human pancreatic cancer. Clin Cancer Res. 2014; 20:3422–33.
https://doi.org/10.1158/1078-0432.CCR-13-2972
PMID:24763614

49. Wolf K, Te Lindert M, Krause M, Alexander S, Te Riet J, Willis AL, Hoffman RM, Figdor CG, Weiss SJ, Friedl P. Physical limits of cell migration: control by ECM space and nuclear deformation and tuning by proteolysis and traction force. J Cell Biol. 2013; 201:1069–84.
https://doi.org/10.1083/jcb.201210152
PMID:23798731

50. Johnson LA, Jackson DG. Hyaluronan and Its Receptors: Key Mediators of Immune Cell Entry and Trafficking in the Lymphatic System. Cells. 2021; 10:2061.
https://doi.org/10.3390/cells10082061 PMID:34440831

51. Alaniz L, Garcia M, Rizzo M, Piccioni F, Mazzolini G. Altered hyaluronan biosynthesis and cancer progression: an immunological perspective. Mini Rev Med Chem. 2009; 9:1538–46.
https://doi.org/10.2174/138955709790361485
PMID:20205635

52. Hallmann R, Zhang X, Di Russo J, Li L, Song J, Hannocks MJ, Sorokin L. The regulation of immune cell trafficking by the extracellular matrix. Curr Opin Cell Biol. 2015; 36:54–61.
https://doi.org/10.1016/j.ceb.2015.06.006
PMID:26189064

53. Lorusso G, Rüegg C, Kuonen F. Targeting the Extra-Cellular Matrix-Tumor Cell Crosstalk for Anti-Cancer Therapy: Emerging Alternatives to Integrin Inhibitors. Front Oncol. 2020; 10:1231.

https://doi.org/10.3389/fonc.2020.01231
PMID:32793493

54. Zou Y, Chen B. Long non-coding RNA HCP5 in cancer. Clin Chim Acta. 2021; 512:33–9.
https://doi.org/10.1016/j.cca.2020.11.015
PMID:33245911

55. Klemm F, Joyce JA. Microenvironmental regulation of therapeutic response in cancer. Trends Cell Biol. 2015; 25:198–213.
https://doi.org/10.1016/j.tcb.2014.11.006
PMID:25540894

56. Liang H, Li X, Wang B, Chen B, Zhao Y, Sun J, Zhuang Y, Shi J, Shen H, Zhang Z, Dai J. A collagen-binding EGFR antibody fragment targeting tumors with a collagen-rich extracellular matrix. Sci Rep. 2016; 6:18205.
https://doi.org/10.1038/srep18205
PMID:26883295

57. Hingorani SR, Zheng L, Bullock AJ, Seery TE, Harris WP, Sigal DS, Braiteh F, Ritch PS, Zalupski MM, Bahary N, Oberstein PE, Wang-Gillam A, Wu W, et al. HALO 202: Randomized Phase II Study of PEGPH20 Plus Nab-Paclitaxel/Gemcitabine Versus Nab-Paclitaxel/ Gemcitabine in Patients With Untreated, Metastatic Pancreatic Ductal Adenocarcinoma. J Clin Oncol. 2018; 36:359–66.
https://doi.org/10.1200/JCO.2017.74.9564
PMID:29232172
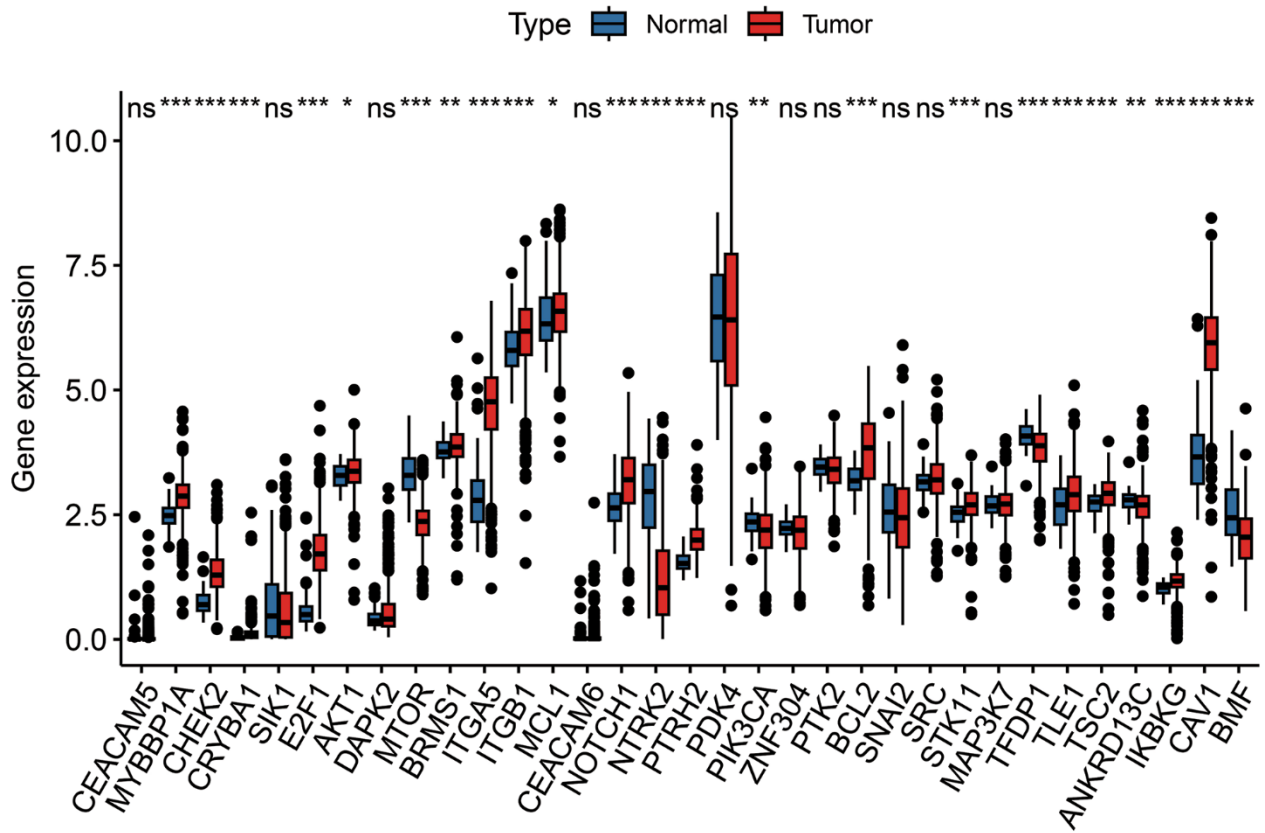
Supplementary Figure 1. The expression profiler of anoikis-related genes in normal and ccRCC samples.

Supplementary Tables

Supplementary Table 1. The gene list of anoikis-related gene signature.

CEACAM5
MYBBP1A
CHEK2
CRYBA1
SIK1
TLE5
E2F1
AKT1
DAPK2
MTOR
BRMS1
ITGA5
ITGB1
MCL1
CEACAM6
NOTCH1
NTRK2
PTRH2
PDK4
PIK3CA
ZNF304
PTK2
BCL2
SNAI2
SRC
STK11
MAP3K7
TFDP1
TLE1
TSC2
ANKRD13C
IKBKG
CAV1
BMF

Supplementary Table 2. Identification of anoikis-related lncRNAs.

AL356599.1
AC012615.6
AL031714.1
AL139287.1
AC005034.5
AC124312.2
AL121832.2
AL731577.2
AL162586.1
LINC01023
AP001505.1
AL136084.3
AC138028.4
AC114730.3
AC011472.1
AC027601.2
NORAD
RUSC1-AS1
AC108449.2
AL022328.2
AC022150.2
AP001486.2
PAXIP1-AS2
OIP5-AS1
AC103809.1
Z68871.1
AC093278.2
RAP2C-AS1
AC023509.4
AC084018.1
AL022322.1
AC008735.2
AC107375.1
AL133215.2
AC108693.2
AC040169.1
HID1-AS1
AC073073.2
AL022328.1
AC109460.2
ZSCAN16-AS1
AL355803.1
CACTIN-AS1
AC092611.2